European Journal of Nuclear Medicine and Molecular Imaging (2021) 48:123–133
https://doi.org/10.1007/s00259-020-04846-3

ORIGINAL ARTICLE

Impact of forced diuresis with furosemide and hydration on the halo artefact and intensity of tracer accumulation in the urinary bladder and kidneys on [^{68}Ga]Ga-PSMA-11-PET/CT in the evaluation of prostate cancer patients

Christian Uprimny[1] · Steffen Bayerschmidt[1] · Alexander Stephan Kroiss[1] · Josef Fritz[2] · Bernhard Nilica[1] · Anna Svirydenka[1] · Clemens Decristoforo[1] · Gianpaolo di Santo[1] · Elisabeth von Guggenberg[1] · Wolfgang Horninger[3] · Irene Johanna Virgolini[1]

Received: 27 February 2020 / Accepted: 28 April 2020 / Published online: 8 May 2020

Abstract

Purpose to assess the influence of intravenous hydration and forced diuresis with furosemide in two different dosages (20 vs 40 mg) on the intensity of tracer accumulation in the urinary collection system and on the occurrence of halo artefact surrounding the urinary bladder and kidneys in [^{68}Ga]Ga-PSMA-11-PET/CT scans.

Materials and methods Comparison of four groups with 50 patients each, receiving different preparation prior to [^{68}Ga]Ga-PSMA-11-PET/CT. Group one, no preparation. Group two, 500 ml sodium chloride administered immediately after tracer injection. Group three, 500 ml sodium chloride and injection of 20 mg furosemide immediately after tracer administration. Group four, 500 ml sodium chloride and injection of 40 mg furosemide immediately after tracer injection. Images were judged visually whether halo artefact was present; semiquantitative measurements were performed with standardised uptake value (SUV).

Results Halo artefact of the urinary bladder was present in twelve patients without preparation, in eight patients receiving only sodium chloride, in one patient injected with 20 mg furosemide/sodium chloride and in two patients receiving 40 mg furosemide/sodium chloride, showing a median SUV_{mean} in the bladder of 45.8, 14.4, 4.6 and 5.8, respectively. Differences between patient group without preparation and the two groups with furosemide/sodium chloride were statistically significant. Patient groups receiving 20 mg furosemide and 40 mg furosemide did not differ significantly. Renal halo artefacts were observed in 15 patients of group one, in ten patients of group two, in 14 patients of group three and in 14 patients of group four, with corresponding median SUV_{mean} values of 33.9, 32.0, 37.8 and 30.4 (no statistically significant differences).

Conclusion Performing [^{68}Ga]Ga-PSMA-11-PET/CT, intravenous injection of 20-mg furosemide and 500-ml sodium chloride significantly reduces the number of bladder halo artefacts and intensity of tracer accumulation in the urinary bladder. A total of 40 mg furosemide does not further improve results.

Keywords Prostate cancer · PET, PET/CT · Prostate-specific membrane antigen · [^{68}Ga]Ga-PSMA-11 · Furosemide · Forced diuresis · Halo artefact · Tracer accumulation in urinary bladder and kidney

Christian Uprimny and Steffen Bayerschmidt contributed equally to this work.

This article is part of the Topical Collection on Oncology - Genitourinary

✉ Christian Uprimny
christian.uprimny@tirol-kliniken.at

[1] Department of Nuclear Medicine, Medical University Innsbruck, Anichstrasse 35, 6020 Innsbruck, Austria

[2] Department of Medical Statistics, Informatics and Health Economics, Medical University Innsbruck, Innsbruck, Austria

[3] Department of Urology, Medical University Innsbruck, Innsbruck, Austria

Introduction

In the past few years, PET/CT with ligands targeting the prostate-specific membrane antigen (PSMA) has emerged as a very powerful imaging technique in the diagnostic work-up of prostate cancer (PC) patients [1–5]. Several PSMA-ligands for PET imaging have been developed and are available for clinical use [6]. [^{68}Ga]Ga-PSMA-11, a PSMA inhibitor, was the first PSMA ligand for PET that was introduced into clinical practice in 2011 and currently represents the most frequently used PSMA tracer worldwide [7]. Despite the well-established high potential of [^{68}Ga]Ga-PSMA-11-PET/CT (in the following referred to as PSMA-11-PET/CT) in detecting tumour lesions in PC patients at different stages of disease [1–5], physiologically high tracer accumulation in the urinary collection system is a well-known problem in the assessment of anatomical structures that are adjacent to the urinary bladder [8–10]. In particular, local recurrences might be missed in PC patients with biochemical relapse mostly due to the masking effect of urinary bladder activity [11]. In this respect, PSMA tracers with little physiologic uptake in the bladder, such as [^{18}F]F-PSMA-1007, seem to be advantageous [12]. In addition, in PSMA-11 PET/CT evaluation of structures adjacent to the urinary collection system may be hampered by the so-called halo artefact that was first described for PSMA-imaging in PET/MRI [9, 10, 13–16]. The halo artefact, also referred to as photopenic artefact or washout artefact, represents an extinction of PET-signal surrounding structures with high tracer uptake. The severity of the halo artefact is positively correlated to high organ-to-background activity ratios [14]. In PSMA-11- PET/CT, this phenomenon is predominantly found around the kidneys and the urinary bladder, the organs with the highest physiologic tracer accumulation [7, 9, 10, 16, 17]. A significant reduction of halo artefacts can be achieved by using modified scatter correction algorithms [15]. For PET/MRI hybrid scanners, a significant reduction of halo artefacts is described if the arms are elevated during exam, most likely due to arm truncation when positioning arms down [18].

In PSMA-11-PET/CT, several strategies can be applied to improve diagnostic certainty in areas surrounding the urinary bladder. Early PET imaging at a timepoint with still low tracer uptake in the urinary tract may help to differentiate malignant PC lesions from urinary bladder activity [13]. However, these techniques require additional imaging.

It has been shown that intensity of urinary bladder activity in PSMA-11-PET/CT can be reduced significantly with administration of diuretics on standard imaging 60 min p.i. but also on late scans with image acquisition 90 min, 120 min and 180 min p.i. [9, 19–23]. In fact, injection of 20 mg furosemide combined with oral hydration of 500 ml water is recommended in the joint EANM and SNMMI procedure guideline for [^{68}Ga]Ga-PSMA-11-PET/CT [6]. However, to date, the possible impact of different patient preparations including forced diuresis and hydration alone on the frequency of halo artefact in PSMA-11-PET/CT was not investigated systematically. In addition, comparative data, whether a higher dosage of furosemide (40 mg) might be more effective in reducing tracer activity in the urinary collecting system than a low-dose protocol with 20 mg of furosemide, is missing. Therefore, in the present study, we examined systematically the influence of two different dosages of furosemide (20 vs 40 mg) combined with hydration on (1) intensity of tracer uptake in the kidneys and urinary bladder and (2) occurrence of halo artefacts around the urinary bladder and kidneys 60 min p.i. in comparison with hydration alone and no intervention prior to imaging.

Materials and methods

Patients

For this retrospective analysis, a total of 424 PC patients who were referred to our department between 6 April 2017 and 26 January 2018 for PSMA-11-PET/CT were extracted from our database. Of these patients, 200 patients were included in the analysis, with four subgroups comprising 50 patients each. Fourteen patients were scanned twice, one patient three times. Patients of group one (G1) received no preparation. Patients of group two (G2) were hydrated intravenously with 500 ml sodium chloride (NaCl 0.9%), starting shortly after tracer injection. Patients of group three (G3) were injected with 20 mg furosemide immediately after tracer application followed by intravenous hydration with 500 ml NaCl 0.9% whereas patients of group four (G4) received 40 mg furosemide intravenously immediately after tracer injection combined with 500 ml NaCl 0.9%. An overview of the four types of preparation procedures is given in Fig. 1. Search for patients in our archive centred on the date, when administration of furosemide and hydration in accordance with the joint EANM/SNMMI guideline was introduced in our clinical routine on 15 May 2017. Until that timepoint, we did not use any preparation (for group one, the last 50 patients without preparation examined before 15 May 2017 were included). Initially we injected 40 mg furosemide combined with NaCl 0.9%, as this represents also our standard dose in renal scintigraphy. However, we soon realised that this dosage caused strong urinary urge during imaging in a quite high number of patients (as stated below in the manuscript). Thus, we decided to reduce dosage after 56 patients (of whom the first 50 patients were included in group four). From 26 June 2017, patients were routinely injected with 20 mg furosemide and 500 ml NaCl 0.9% as a standard protocol (group three comprises the first 50 patients who received this preparation). For group two, we extracted those patients from the database who did not consent to injection of furosemide. In that case, they

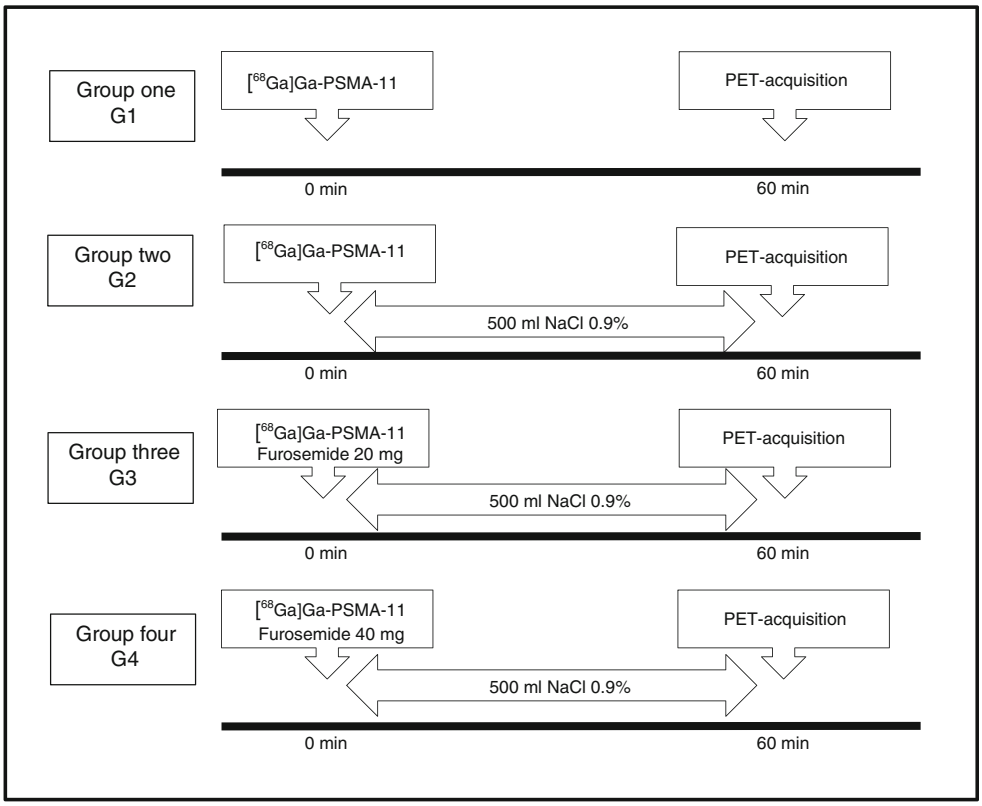

Fig. 1 Overview of four different preparation protocols G1–G4

received only hydration with 500 ml NaCl 0.9%. The first patient with NaCl 0.9% only was identified on 24 May 2017, patient number 50 on 26 January 2018. In the mixed cohort study, indications for PSMA-11-exams were as follows: primary diagnosis ($n = 5$, median PSA 5.89 ng/ml, range 0.47–158), primary staging ($n = 13$, median PSA 13.37, range 0.12–92.8), biochemical recurrence/PSA-persistence after primary therapy ($n = 132$; median PSA 1.63 ng/ml, range 0.09–574.7), evaluation of therapy response/restaging ($n = 50$; median PSA 5.9 ng/ml, range 0.04–490.7). Further patient characteristics of the different preparation groups are listed in Table 1.

Radiopharmaceutical

PSMA-11 (Glu-NH-CO-NH-Lys(Ahx)-HBED-CC; HBED=*N,N′*-bis[2-hydroxy-5-(carboxyethyl)benzyl]ethylenediamine-N, N′-diacetic acid) was obtained from ABX advanced biochemical compounds (Radeberg, Germany) in GMP quality. [^{68}Ga]Ga-PSMA-11 was prepared on an automated synthesis module (Modular-Lab PharmTracer; Eckert & Ziegler, Berlin) using a procedure previously described [13, 24]. The radiochemical purity of the final product was > 91% as analysed by reversed phase HPLC analysis and TLC proving the absence of colloidal ^{68}Ga.

Imaging protocol

PSMA-11 PET/CT imaging was conducted using a dedicated PET/CT system in time of flight mode (Discovery 690; GE Healthcare, Milwaukee, WI). Sixty minutes after injection of [^{68}Ga]Ga-PSMA-11 (median activity 164 MBq; range 122–216 MBq), a whole-body PET scan (skull vertex to upper thighs) in three-dimensional mode was acquired (emission time, 2 min per bed position with an axial field-of-view of

Table 1 Patient characteristics by different preparation groups G1–G4

	G1 ($n = 50$)	G2 ($n = 50$)	G3 ($n = 50$)	G4 ($n = 50$)
PSA ng/ml median (range)	3.3 (0.06–364)	5.57 (0.21–574.7)	0.86 (0.04–50.9)	1.98 (0.05–158)
Activity MBq median (range)	164.5 (122–200)	164.0 (136–200)	173 (131–216)	166 (132–198)
Uptake time min median (range)	72.5 (53–105)	65 (58–97)	68 (51–97)	73 (52–101)
Arms up	38 (76.0%)	41 (82.0%)	38 (76.0%)	40 (80.0%)
Glomerular filtration rate*, < 60 ml/min/1.73m^2	14.0%	18.0%	16.0%	16.0%

* p value for overall group comparison G1–G4; $p = 0.972$

15.6 cm per bed position). Variation of injected [^{68}Ga]Ga-PSMA-11 activity was due to the short half-life of ^{68}Ga and variable elution efficiencies of the ^{68}Ge/^{68}Ga radionuclide generator. However, image quality of PET scans in patients in whom lower activities were administered was good and judged sufficient for correct image analysis. A total of 122 patients (61%) received a diagnostic contrast-enhanced CT (ceCT) scan. The ceCT scan parameters using "GE smart mA dose modulation" were as follows: 100 or 120 kVp, 80–450 mA, noise index 24, 0.8 s per tube rotation, slice thickness 3.75 mm and pitch 0.984. A CT scan of the thorax, abdomen and pelvis (shallow breathing) was acquired 40–70 s after injection of contrast agent (60 to 120 ml of Iomeron 400 mg/l, depending on patient body weight), followed by a CT scan of the thorax in deep inhalation. In the remaining 78 patients (39%), a low-dose CT scan was performed for attenuation correction of the PET emission data. Low-dose CT images were also used for anatomical correlation of lesions with increased uptake found on PET. The low-dose CT scan parameters using "GE smart mA dose modulation" were as follows: 100 kVp, 15–150 mA, noise index 60, 0.8 s per tube rotation, slice thickness 3.75 mm and pitch 1.375. Reconstruction was performed with an ordered subset expectation maximization algorithm (OSEM) with 4 iterations/8 subsets. Images were also corrected for randoms and scatter using a software with an integrated correction algorithm provided and predefined by the vendor. In 157 patients (78.5%), examination was performed in an arms up position whereas in 43 patients (21.5%), scans were acquired with arms down. Prior to start of image acquisition, patients were asked to void the bladder and encouraged to insert an adult diaper liner provided by our institution to prevent possible contamination of clothes and scanner gantry in case of urinary urgency.

Image analysis

All PSMA-11-PET/CT images were analysed with dedicated commercially available software (GE Advance Workstation SW Version AW4.5 02), which allowed the review of PET, CT and fused imaging data in axial, coronal and sagittal slices. PET images were interpreted independently by two board-approved nuclear medicine physicians with more than 10 years of clinical experience, who were blinded to the method of patient preparation prior to the exam. In a first step, PET images were assessed on all three planes (axial, sagittal, coronal) whether halo artefacts were present around the kidneys and the urinary bladder. In case of disagreement between the two readers, images were reevaluated and a consensus was reached in a second round. In addition, for quantification of tracer activity in the urinary collection system, mean and maximum standardized uptake values (SUV_{mean}, SUV_{max}) of each kidney and the urinary bladder were calculated, applying volumes of interest (VOIs) that were drawn automatically with a manually adapted isocontour threshold centred on the organs of interest.

Statistical analysis

Variables of interest were compared between treatment groups using non-parametric testing procedures. Specifically, median SUV_{max} values were compared between groups using the Kruskal-Wallis rank sum test [25], and probabilities of halo artefacts using Fisher's exact test. In case of statistically significant findings, pairwise group comparisons (Dunn's test; Fisher's exact test) were performed [26], correcting the resulting p values according to the Bonferroni-Holm method to counteract the problem of multiple comparisons [27]. For testing for differences in SUV_{max} values between patients presenting with vs without halo artefact, we used the Scheirer–Ray–Hare test adjusting for treatment group [28], in addition to univariate Mann-Whitney U tests. For testing the association of arm position and the probability of halo artefacts, we used the Cochran–Mantel–Haenszel test adjusted for treatment group. All tests of statistical significance were two-sided, and p-values less than 0.05 were considered statistically significant. All analyses were conducted in the R, version 3.5.1. [29]

Results

Comparing the four different groups with respect to tracer accumulation in the urinary bladder, intensity of tracer accumulation was highest without any preparation (G1) showing a median SUV_{mean} of 45.8 (range 5.9–237.0). With intravenous injection of 500 ml NaCl 0.9% (G2), tracer uptake in the bladder could be reduced, showing a median SUV_{mean} of 14.4 (range 5.1–116.4). Combination of hydration with 500 ml NaCl 0.9% and 20 mg or 40 mg furosemid (G3 and G4) led to a decrease of tracer accumulation in the bladder with a median SUV_{mean} of 4.6 (range 1.4–23.4) and 5.8 (range 1.2–29.7), respectively. The differences between the group without preparation on the one hand and the three subgroups G2, G3 and G4 were statistically significant ($p < 0.001$ and $p = 0.009$). A statistically significant reduction could also be found between patients of group G2 with 500 ml NaCl 0.9% and group G3 with 500 ml NaCl 0.9% + 20 mg furosemid as well as group G4 with 500 ml NaCl 0.9% + 40 mg furosemid ($p < 0.001$). There was no statistically significant difference in SUV_{mean} values between 500 ml NaCl 0.9% + 20 mg furosemid and 500 ml NaCl 0.9% + 40 mg furosemide ($p = 0.509$).

Regarding tracer uptake in the kidney, a median SUV_{mean} of 33.9 (range 8.1–66.1) was found in the subgroup without intervention. Patients in subgroup G2 showed a slightly lower kidney accumulation with a median SUV_{mean} of 32.0 (range 6.8–63.5), not reaching a statistical significant difference ($p =$ 1). Renal uptake was highest in subgroup G3 with a median

SUV_{mean} of 37.8 (range 22.7–57.7). In subgroup G4, uptake in kidneys was almost equal to G1 (median SUV_{mean} 30.4; range 18.4–61.5). An overview of SUV_{mean} but also SUV_{max} values and statistical analysis of different subgroups with calculated *p* values is given in Tables 2 and 3.

A halo artefact around the bladder region could be detected in a total of 23 patients (11.5%). Subgroup G1 with no intervention (12 patients, 24.0%) and subgroup G2 with hydration alone (eight patients, 16.0%) accounted for the majority of cases. In contrast, halo artefact caused by the bladder was present in only one patient of subgroup G3 with 20 mg furosemide (2.0%) and two patients in subgroup G4 with 40 mg furosemide (4.0%). Reduction of frequency in halo artefacts of the bladder was strongest between group G1 and group G3 and group G4, reaching also statistical significance ($p < 0.001$ each). Compared with G1 (receiving no intervention), a statistically significant reduction could not be achieved with hydration alone ($p = 0.908$ for G1 vs G2). Although number of bladder halo artefacts was lower in group G3 and group G4 in comparison with group G2, no statistically significant difference could be observed between these subgroups either ($p = 0.123$ for G2 vs G3 and $p = 0.275$ for G2 vs G3).

A total of 53 patients (26.5%) did show a halo artefact in the kidney region. Kidney halo artefact could be observed in 15 patients of subgroup G1 (30.0%), in ten patients of subgroup G2 (20.0%), in 14 patients of subgroup G3 (28.0%) and in 14 patients in subgroup G4 (28.0%). No statistically significant difference between the four groups was found (overall *p* value = 0.666). For a synopsis of details on halo artefacts and respective statistical analysis, please refer to Tables 4 and 5.

Intensity of urinary bladder activity was significantly associated with the occurrence of halo artefacts around the bladder. Patients with a bladder halo artefact showed a significantly higher SUV_{mean} of the urinary bladder than patients without a halo artefact (median SUV_{mean} 65.4 vs 8.4; $p = 0.003$). On the other hand, no significant difference between SUV_{mean} values could be found between patient subgroups with and without halo artefacts surrounding the kidneys (median SUV_{mean} 32.8 vs 34.9; $p = 0.716$). Respective data are presented in Table 6.

Arm positioning during scan acquisition did not exert a statistically significant effect on the frequency of halo artefacts of the bladder (14.0% of patients with arms down vs 10.8% of patients with arms up; $p = 0.579$). In contrast, the number of halo artefacts around the kidneys was significantly higher in patients with arms down compared with patients with arms up (55.8 vs 18.5% of patients; $p < 0.001$), see Table 7).

We also assessed intensity of tracer uptake in the parotid gland, an organ with high physiologic PSMA-11

Table 3 Results of pairwise group comparison of intensity of tracer accumulation in urinary bladder and kidneys according to Dunn's test, corrected for multiple testing. Group one (G1): no intervention. Group two (G2): intravenous application of 500 ml NaCl 0.9%. Group three (G3): 20 mg furosemide and 500 ml NaCl 0.9% intravenously. Group four (G4): 40 mg furosemide and 500 ml NaCl 0.9% intravenously

	G1	G2	G3	G4
SUV_{max} bladder				
G1	–	0.006	< 0.001	< 0.001
G2	0.006	–	< 0.001	< 0.001
G3	< 0.001	< 0.001	–	0.528
G4	< 0.001	< 0.001	0.528	–
SUV_{mean} bladder				
G1	–	0.009	< 0.001	< 0.001
G2	0.009	–	< 0.001	< 0.001
G3	< 0.001	< 0.001	–	0.509
G4	< 0.001	< 0.001	0.509	–
SUV_{mean} kidneys				
G1	–	1	0.125	0.796
G2	1	–	0.02	1
G3	0.125	0.02	–	0.079
G4	0.796	1	0.079	–

Table 2 Comparison of intensity of tracer accumulation in urinary bladder and kidneys expressed in maximum and mean standardized uptake values (SUV_{max}, SUV_{mean}) between four subgroups with different patient preparation. Group one (G1), no intervention. Group two (G2), intravenous application of 500 ml NaCl 0.9%. Group three (G3), 20 mg furosemide and 500 ml NaCl 0.9% intravenously. Group four (G4), 40 mg furosemide and 500 ml NaCl 0.9% intravenously

	G1	G2	G3	G4	*p* value*
SUV_{max} median bladder	68.4	23.1	8.9	9.6	< 0.001
SUV_{max} range bladder	9.3–350.0	9.0–170.6	2.3–32.1	2.3–26.8	–
SUV_{mean} median bladder	45.8	14.4	4.6	5.8	< 0.001
SUV_{mean} range bladder	5.9–237.0	5.1–116.4	1.4–23.4	1.2–29.7	–
SUV_{max} median kidneys	51.7	47.2	61.0	51.6	< 0.001
SUV_{max} range kidneys	13.6–127.5	11.5–78.8	38.6–90.9	20.9–91.4	–
SUV_{mean} median kidneys	33.9	32.0	37.8	30.4	0.018
SUV_{mean} range kidneys	8.1–66.1	6.8–63.5	22.7–57.5	18.4–61.5	–

* *p* values for overall group comparison from Kruskal-Wallis rank sum test

Table 4 Number (*n*) of patients with halo artefact around urinary bladder and surrounding kidneys in subgroups with different type of patient preparation. Group one (G1), no intervention. Group two (G2), intravenous application of 500 ml NaCl 0.9%. Group three (G3), 20 mg furosemide and 500 ml NaCl 0.9% intravenously. Group four (G4), 40 mg furosemide and 500 ml NaCl 0.9% intravenously. In addition, number (*n*) of patients with urge to urinate in different groups is listed

	G1	G2	G3	G4	*p* value*
Halo artefact bladder *n* (%)	12 (24.0)	8 (16.0)	1 (2.0)	2 (4.0)	0.001
Halo artefact kidneys *n* (%)	15 (30.0)	10 (20.0)	14 (28.0)	14 (28.0)	0.666
Urinary urgency *n* (%)	3 (6.0)	2 (4.0)	20 (40.0)	24 (48.0)	–

* *p* values for overall group comparison from Fisher's exact test

accumulation, showing a median SUV_{mean} value in the four groups of 11.8, 11.6, 11.8 and 12.5, respectively (no statistically significant difference; $p = 0.582$).

Patients were also questioned whether they felt urinary urgency during PET/CT acquisition, categorizing it as slight, moderate (tolerable) and strong (major discomfort). In subgroups G1 and G2, a slight urgency occurred in only three (6%) and two patients (4%), respectively. In subgroups G3 with 20 mg furosemide, 20 patients (40%) stated a slight to moderate urge to urinate. In subgroup G4 using 40 mg furosemide, 24 patients (48%) had a urinary urgency that was classified strong in nine cases and caused an interruption of the exam in two patients due to urination.

Preliminary results of this analysis were presented on the EANM congress 2019 in Barcelona. The corresponding abstract can be accessed at https://link.springer.com/content/pdf/10.1007/s00259-019-04486-2.pdf (OP-039).

Discussion

In PSMA-11-PET/CT, assessment of anatomic structures in the vicinity of the urinary bladder and kidneys can be disturbed to a great extent by intense urinary tracer accumulation, causing also the appearance of halo artefacts around these organs (as displayed on Fig. 2). Halo artefacts in particular are a drawback in PET/MRI hybrid imaging; however, phantom studies could show that this phenomenon is not strictly modality-dependant and also occurs on PET/CT scanners [14]. The halo artefact is considered to be mostly due to an overcorrection of scatter caused by scatter correction algorithms, usually integrated in image reconstruction of modern PET/CT systems [14]. In general, scatter correction models applied in image reconstruction of modern PET/CT systems were developed for ^{18}F-tracers and have the tendency to overestimate scatter on scans with ^{68}Ga-labelled tracers [15]. Regions with high uptake have a high level of scatter in comparison with surrounding tissue with low tracer uptake. If scatter estimation using these algorithms is erroneous, a halo artefact may be produced on images with ^{68}Ga-tracers in areas with high tracer accumulation such as the urinary bladder and kidneys [15]. The phenomenon of halo artefact is known in PET scans using ^{68}Ga-labelled PSMA-ligands but is also described in other ^{68}Ga-labelled compounds such as DOTATOC [30]. Algorithms with modified parameters, primarily increasing the number of axial subsamples, seem to result in a more accurate scatter correction in ^{68}G-labelled tracers such as PSMA-11, reducing the frequency of halo artefacts [15, 16]. However, scatter correction usually is an integrated part of the reconstruction algorithms provided by the manufacturers, and adjusting reconstruction parameters on site requires high expertise and is usually not performed by most institutions, as it is the case at our department. Reconstruction of images with time of flight information, as it was also the case in all of our exams, seems to have a positive influence on the size of halo artefacts but not on the frequency of this phenomenon [14].

It has been shown that occurrence of halo artefacts in general is positively correlated with intensity of tracer accumulation and high organ to background ratios, which is particularly the case in the bladder region on PSMA-11-PET scans [14]. Our findings confirm that the frequency of halo artefacts in the bladder region is clearly associated with intensity of tracer uptake in the urinary bladder. We found significantly higher SUV-values in the bladder in patients with halo artefacts in comparison with patients without halo artefacts (median SUV_{max} 94.4 vs 14.3).

Table 5 Results of pairwise group comparison regarding number of halo artefacts around urinary bladder, according to Fisher's exact test, corrected for multiple testing. As the overall *p* value for halo artefacts in the kidneys was 0.666, demonstrating no overall statistical difference, pairwise group comparisons was not performed for halo artefacts in the kidney. Group one (G1), no intervention. Group two (G2), intravenous application of 500 ml NaCl 0.9%. Group three (G3), 20 mg furosemide and 500 ml NaCl 0.9% intravenously. Group four (G4), 40 mg furosemide and 500 ml NaCl 0.9% intravenously

Halo artefact bladder	G1	G2	G3	G4
G1	–	0.908	0.011	0.038
G2	0.908	–	0.123	0.275
G3	0.011	0.123	–	1.000
G4	0.038	0.275	1.000	–

Table 6 Comparison of intensity of tracer accumulation in the urinary bladder and kidneys expressed as SUV_{max} and SUV_{mean} with number of halo artefacts surrounding bladder and kidneys

	Halo artefact bladder, no ($n = 177$)	Halo artefact bladder, yes ($n = 23$)	p value*
SUV_{max} median (range) bladder	14.3 (2.3–242.2)	94.4 (15.0–350.0)	$p < 0.001$ (unadjusted), $p = 0.003$ (adjusted for treatment group)
SUV_{mean} median (range) bladder	8.4 (1.2–212.0)	65.4 (9.4–237.0)	$p < 0.001$ (unadjusted), $p = 0.003$ (adjusted for treatment group)
	Halo artefact kidney, no ($n = 147$)	Halo artefact kidney, yes ($n = 53$)	p value*
SUV_{max} median (range) kidney	54.7 (11.5–127.5)	50.9 (22.3–91.4)	$p = 0.560$ (unadjusted), $p = 0.421$ (adjusted for treatment group)
SUV_{mean} median (range) kidney	34.9 (6.8–66.1)	32.8 (15.2–61.5)	$p = 0.716$ (unadjusted), $p = 0.621$ (adjusted for treatment group)

* Mann-Whitney U test for unadjusted p value, and Scheirer–Ray–Hare test for adjusted p value

As application of different scatter correction algorithms is technically challenging, the main aim of this study was to clarify whether patient preparation influencing tracer accumulation in the urinary collection system has the potential to diminish the frequency of halo artefacts. In fact, with regard to the urinary bladder, subgroup analysis of our data showed that number of halo artefacts was highest in patients without preparation ($n = 12$). Intravenous hydration alone showed a decrease of halo artefact ($n = 8$); however, it did not reach statistical significance. Administration of furosemide could reduce the number of halo artefacts significantly, in particular, in comparison with patients without intervention but also compared with patients receiving intravenous hydration alone. In the subgroups with injection of 20 and 40 mg furosemide, a halo artefact of the bladder was present in only one and two patients, respectively. Of note, 40 mg furosemide was not superior to a low-dose diuretic protocol with 20 mg furosemide, while leading to a stronger urge to urinate.

Examining the influence of forced diuresis and hydration on intensity of tracer accumulation in the urinary bladder, we could show that hydration alone can reduce bladder activity significantly in comparison with no intervention (median SUV_{max} 23.1 vs 68.4). The highest reduction of tracer uptake in the bladder could be achieved with a combination of hydration and furosemide. The results on forced diuresis go in line with previously published data. A positive correlation of administration of furosemide and reduced tracer accumulation of ^{68}Ga-labelled PSMA-ligands in the bladder on delayed imaging 90 min, 120 min and 180 min p.i. was already described [20–23]. In a study by Fennessy et al. comprising 62 PC patients, authors could demonstrate a significant reduction of tracer accumulation in the urinary bladder and ureters also on PET images acquired 60 min p.i. in the subgroup of patients that received 20 mg furosemide concurrently with tracer injection in comparison with patients without intervention [19]. However, in none of the aforementioned studies, a comparison of patients receiving furosemide with a cohort of patients with hydration alone was performed, nor was the question addressed whether a higher dosage of furosemide could be more effective than administration of low-dose furosemide. In our study, intravenous injection of 40 mg furosemide combined with hydration could not enhance tracer wash out of the bladder compared with 20 mg furosemide and hydration (median SUV_{max} 9.6 vs 8.9). In addition, urinary urgency was markedly more severe in patients injected with 40 mg furosemide than with 20 mg furosemide. Although urinary urgency was also present in 40% of patients receiving 20 mg furosemide, it was only classified by patients as mild to moderate

Table 7 Influence of arm positioning during PET/CT scan on appearance of halo artefact in the urinary bladder and kidney region. Subgroups with arms up ($n = 157$) and arms down ($n = 43$) are compared, and statistical analyses of subgroups with different arm positioning in the respective organ are listed

	Arms up ($n = 157$)	Arms down ($n = 43$)	p value (unadjusted)	p value (adjusted for treatment group)*
Halo artefact kidney yes n (%)	29 (18.5%)	24 (55.8%)	< 0.001	< 0.001
Halo artefact kidney no n (%)	128 (81.5%)	19 (44.2%)		
Halo artefact bladder yes n (%)	17 (10.8%)	6 (14.0%)	0.592	0.579
Halo artefact bladder no n (%)	140 (89.2%)	37 (86.0%)		

* Fisher's exact test for unadjusted p values, and Cochran–Mantel–Haenszel test for adjusted p values

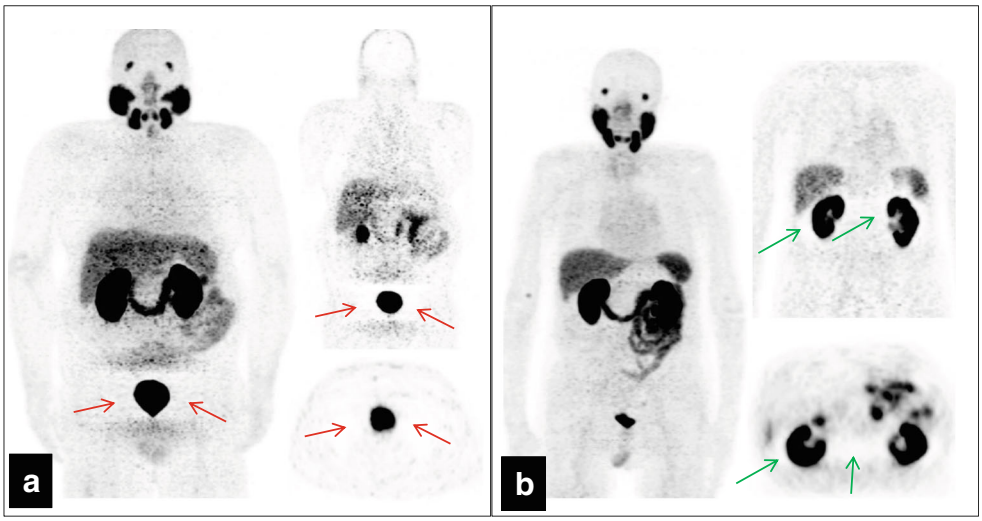

Fig. 2 PET-mages of two prostate cancer patients with biochemical recurrence referred for PSMA-11-PET/CT. Both patients did not receive a preparation with furosemide and hydration prior to imaging. In Fig. 2a, a severe halo artefact is clearly visible around the bladder (SUV_{max} of bladder 141.8), red arrows pointing at the artefact on coronal and axial planes. In Fig. 2b, a halo artefact in the kidney area is depicted (SUV_{max} of kidneys 53.7), green arrows highlighting the artefact on coronal and axial planes

and did not negatively affect image acquisition. The effect of furosemide on tracer accumulation in the bladder is illustrated on Fig. 3**,** displaying a PC patient who underwent sequential PSMA-11-PET/CT without and with furosemide, with local recurrence clearly visible only on images with furosemide.

Accumulation of ^{68}Ga-PSMA-11 in the kidneys is known to be relatively high [7, 17]; however, the issue whether there is also an impact of hydration and forced diuresis on renal uptake has not been investigated to date. Surprisingly in our study, tracer accumulation in the kidneys could not be reduced significantly with hydration or furosemide in comparison with patients not receiving any intervention, showing even the highest SUV_{max} in the subgroup of patients with 20 mg furosemide (median SUV_{max} of 61.0 with 20 mg furosemide vs median SUV_{max} of 54.3 without intervention). This could be partly explainable that ^{68}Ga-PSMA-11 binds with high affinity to the renal tubules, as demonstrated in immunohistochemical analysis [31]. Furosemide only increases tracer excretion in the urinary collecting system but obviously does not influence the binding of the tracer to the tubular structures. An example of the impact of forced diuresis on intensity of tracer accumulation in the urinary bladder and in the kidneys is

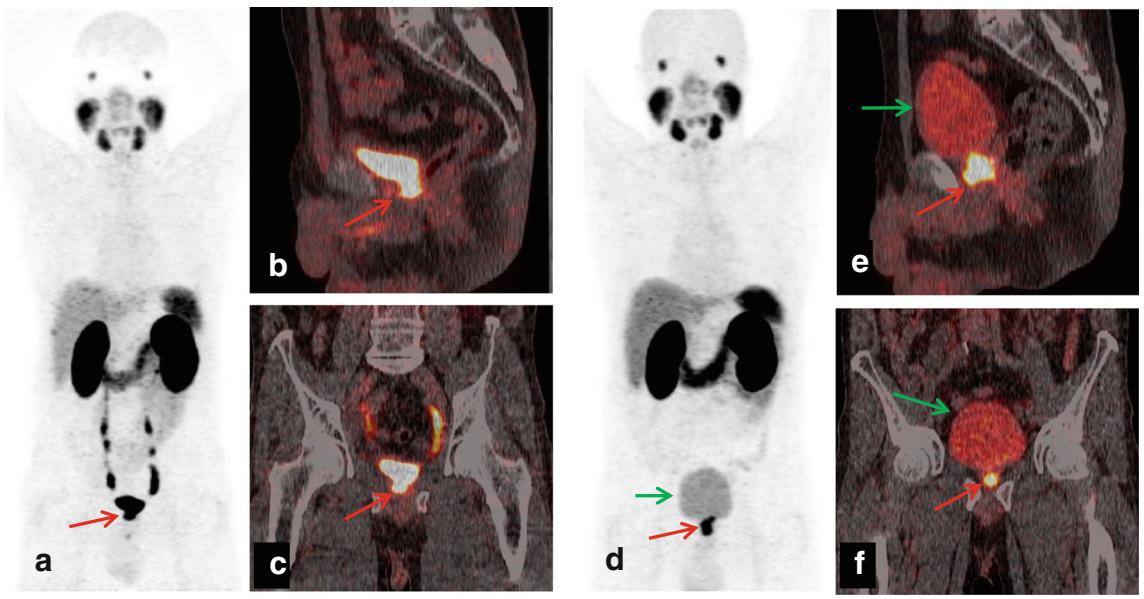

Fig. 3 Prostate cancer patient with biochemical recurrence treated with radical prostatectomy who underwent sequential PSMA-11-PET/CT without preparation in March 2018 (**a** maximum intensity projection and **b**–**c** fused sagittal and coronal planes) and with 20 mg furosemide combined with 500 ml NaCl 0.9% in July 2018 (**d** maximum intensity projection and **b**–**c** fused sagittal and coronal planes). Red arrows in images **a**–**c** point at the bottom of the urinary bladder, where a clear distinction between a local recurrence and tracer accumulation in the neck of the bladder is not possible (SUV_{max} of the bladder 94.8). On subsequent PET scans with forced diuresis, tracer uptake in the urinary bladder is low (SUV_{max} of bladder 5.7), green arrows pointing at the bladder in images **d**–**f**. A local recurrence with a SUV_{max} of 19.9 is now evident (red arrows on images **d**–**f**)

presented in Fig. 4, showing a patient who underwent PSMA-11-PET/CT without and with furosemide.

Noteworthy, in contrast to halo artefact caused by the bladder, occurrence of halo artefact around the kidneys was not influenced by hydration or forced diuresis. In comparison with patients receiving no preparation, we did not find a significant reduction in number of renal halo artefacts with the use of hydration or furosemide, even in the high dosage subgroup. This is probably due to the fact that infusion of 500 ml NaCl 0.9% and administration of furosemide did not cause a significant reduction of tracer accumulation in the kidneys, as described before. As type of patient preparation did not influence the frequency of renal halo artefacts, a higher total number of halo artefact in the kidney region were observed as compared with the urinary bladder ($n = 53$ vs $n = 23$, respectively).

Arm positioning has also been reported to constitute an important factor on the appearance of the halo artefact at least on PET/MRI scans with ^{68}Ga-PSMA-11 [18]. Afshar-Oromieh et al. could demonstrate that putting the arms above the head led to a significant reduction of halo artefacts around the kidneys and the bladder on PSMA-11-PET/MRI in comparison with positioning arms down. The field of view of the MRI is smaller than that of PET, producing false attenuation correction coefficients that can lead to a prominent halo artefact around the kidney and bladder. In PET/CT systems, the field of view of PET and CT is quite similar, and false attenuation correction due to arm truncation should not play a role. In fact, in our patient cohort, we could not find a significant difference in the occurrence of halo artefacts for the bladder between the two groups examined with arms up and arms down (14% of patients with arms down vs 10.8% of patients with arms up). However, surprisingly for the kidney region, a significantly higher number of halo artefacts was observed in patients examined with arms down compared with patients with arms up (55.8% of patients with arms down vs 18.5% of patients with arms up). Although the cause for it remains unclear, our data suggest that there seems to be an influence of arm positioning on the frequency of kidney halo artefacts.

There are some limitations within this study. Firstly, the data were collected retrospectively. In addition, different preparation protocols were introduced sequentially in daily practice. Although readers were blinded to the type of preparation, information on the protocol could have been theoretically identified by the date of the PET scans. This may have introduced some reader bias in reporting halo artefacts. However, we are strongly convinced that the double reading of the scans by two experts with expertise in reporting PSMA-11-PET/CT since 2014 could reduce this possible bias to a minimum. We are also aware of the fact that appearance of halo artefacts is

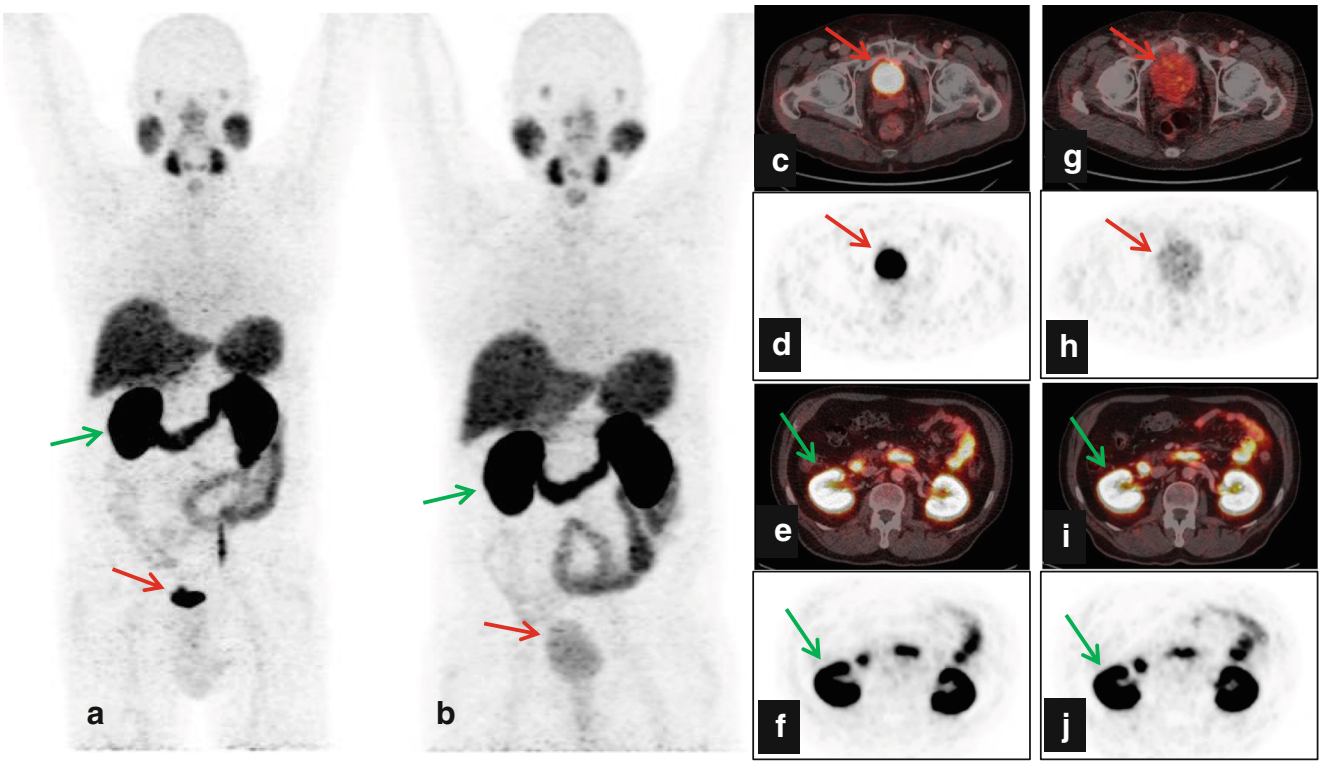

Fig. 4 Sequential PSMA-11-PET/CT scans with different preparation protocols of a prostate cancer patient who was referred for assessment of biochemical recurrence two times within 6 months. Images **a** (maximum intensity projection) and **c**–**f** (axial slices) represent PET/CT scan without preparation, showing high uptake in the bladder (red arrows; SUV_{max} of bladder 77.1) and in the kidneys (green arrows; SUV_{max} of kidneys 49.4). On images **b** (maximum intensity projection) and images **g**–**j** (axial slices), PET/CT scan after intravenous administration of 40 mg furosemide and injection of 500 ml NaCl 0.9% is shown, with a markedly reduced tracer uptake in the bladder (red arrows; SUV_{max} of bladder 8.2), whereas intensity of tracer retention in the kidneys remains almost stable (green arrows; SUV_{max} of kidneys 46.3)

dependant on the type of PET/CT scanner used. Our results reflect the data of a specific scanner (Discovery 690; GE Healthcare) and cannot be necessarily transferred to other PET/CT systems, especially recent generation scanners.

Some concerns may also be raised regarding the early timepoint of furosemide injection. As furosemide was administered shortly after tracer injection, it is not excluded that significant amounts of tracer could be excreted before it binds to the PSMA-receptors, possibly reducing lesion detectability. At least with respect to the parotid gland, an organ with physiologically high PSMA-11 accumulation, we could not find statistically significant differences in intensity of tracer uptake between patients injected with furosemide and patients not receiving furosemide. This could be interpreted as an indirect sign that furosemide-induced wash out is not as pronounced as assumed. However, this issue requires further investigations, ideally with pharmacokinetic studies including measurements of tracer activity in blood and urine at different timepoints of the tracer uptake period.

In summary, in PSMA-11-PET/CT, patient preparation with forced diuresis combined with hydration helps to increase tracer wash out of the urinary bladder and reduces the appearance of halo artefacts in the bladder region significantly. In our experience, combination of 20 mg furosemide and hydration is tolerated well by the patients. Nevertheless, until further studies are available, which prove that administration of furosemide at the timepoint of tracer injection does not cause a relevant wash out of the tracer before binding to PSMA, a simultaneous injection of furosemide and PSMA-11 cannot be generally recommended.

Conclusion

Although forced diuresis with furosemide and hydration does not influence the frequency of halo artefacts around the kidneys, the number of halo artefacts surrounding the bladder and intensity of tracer accumulation in the bladder were significantly reduced with administration of furosemide combined with intravenous hydration. Intravenous injection of 40 mg furosemide did not prove to be more efficient than injection of 20 mg furosemide. However, caution using this protocol with simultaneous injection of furosemide and PSMA-11 is warranted. A risk of tracer wash out of relevant amounts of tracer before it had the possibility to interact with PSMA cannot be excluded. Arms up positioning during scanning is advocated, due to its potential to mitigate the frequency of halo artefacts in the kidney area.

Acknowledgements We want to express our gratitude to all the members of our PET staff for their contribution in performing this study.

Compliance with ethical standards

Conflict of interest The authors declare that they have no conflict of interest.

Ethical approval All procedures performed in this study were in accordance with the ethical standards of the institutional and national research committee and with the principles of the 1964 Declaration of Helsinki and its subsequent amendments [32]. In accordance with our local regulations, ethical approval was waived, as the study was conducted retrospectively from data obtained for clinical purposes. Written informed consent was obtained from all patients prior to the exam, and the retrospective study was conducted according to institutional guidelines and is in compliance with the specific requirements of our country.

References

1. Afshar-Oromieh A, Holland-Letz T, Giesel FL, Kratochwil C, Mier W, Haufe S, et al. Diagnostic performance of 68Ga-PSMA-11 (HBED-CC) PET/CT in patients with recurrent prostate cancer: evaluation in 1007 patients. Eur J Nucl Med Mol Imaging. 2017;44:1258–68. https://doi.org/10.1007/s00259-017-3711-7.
2. Caroli P, Sandler I, Matteucci F, De Giorgi U, Uccelli L, Celli M, et al. 68Ga-PSMA PET/CT in patients with recurrent prostate cancer after radical treatment: prospective results in 314 patients. Eur J Nucl Med Mol Imaging. 2018;45:2035–44. https://doi.org/10.1007/s00259-018-4067-3.
3. Fendler WP, Calais J, Eiber M, Flavell RR, Mishoe A, Feng FY, et al. Assessment of 68Ga-PSMA-11 PET accuracy in localizing recurrent prostate cancer: a prospective single-arm clinical trial. JAMA Oncol. 2019;5:856–63. https://doi.org/10.1001/jamaoncol.2019.0096.
4. Virgolini I, Decristoforo C, Haug A, Fanti S, Uprimny C. Current status of theranostics in prostate cancer. Eur J Nucl Med Mol Imaging. 2018;45:471–95. https://doi.org/10.1007/s00259-017-3882-2.
5. Uprimny C. Ga-PSMA-11 PET/CT: the rising star of nuclear medicine in prostate cancer imaging? Wien Med Wochenschr. 2019;169:3–11. https://doi.org/10.1007/s10354-017-0569-z.
6. Fendler WP, Eiber M, Beheshti M, Bomanji J, Ceci F, Cho S, et al. Ga-PSMA PET/CT: joint EANM and SNMMI procedure guideline for prostate cancer imaging: version 1.0. Eur J Nucl Med Mol Imaging. 2017;44:1014–24. https://doi.org/10.1007/s00259-017-3670-z.
7. Afshar-Oromieh A, Malcher A, Eder M, Eisenhut M, Linhart HG, Hadaschik BA, et al. PET imaging with a [68Ga]gallium-labelled PSMA ligand for the diagnosis of prostate cancer: biodistribution in humans and first evaluation of tumour lesions. Eur J Nucl Med Mol Imaging. 2013;40:486–95. https://doi.org/10.1007/s00259-012-2298-2.
8. Fanti S, Minozzi S, Morigi JJ, Giesel F, Ceci F, Uprimny C, et al. Development of standardized image interpretation for 68Ga-PSMA PET/CT to detect prostate cancer recurrent lesions. Eur J Nucl Med Mol Imaging. 2017;44:1622–35. https://doi.org/10.1007/s00259-017-3725-1.
9. Afshar-Oromieh A, Haberkorn U, Schlemmer HP, Fenchel M, Eder M, Eisenhut M, et al. Comparison of PET/CT and PET/MRI hybrid systems using a 68Ga-labelled PSMA ligand for the diagnosis of recurrent prostate cancer: initial experience. Eur J Nucl Med Mol Imaging. 2014;41:887–97. https://doi.org/10.1007/s00259-013-2660-z.
10. Hofman MS, Hicks RJ, Maurer T, Eiber M. Prostate-specific membrane antigen PET: clinical utility in prostate cancer, normal

patterns, pearls, and pitfalls. Radiographics. 2018;38:200–17. https://doi.org/10.1148/rg.2018170108.
11. Freitag MT, Radtke JP, Afshar-Oromieh A, Roethke MC, Hadaschik BA, Gleave M, et al. Local recurrence of prostate cancer after radical prostatectomy is at risk to be missed in 68Ga-PSMA-11-PET of PET/CT and PET/MRI: comparison with mpMRI integrated in simultaneous PET/MRI. Eur J Nucl Med Mol Imaging. 2017;44:776–87. https://doi.org/10.1007/s00259-016-3594-z.
12. Giesel FL, Will L, Lawal I, Lengana T, Kratochwil C, Vorster M, et al. Intraindividual comparison of 68Ga-PSMA-11-PET/CT and multiparametric MR for imaging of primary prostate cancer. J Nucl Med. 2018;59:1076–80. https://doi.org/10.2967/jnumed.117.204669.
13. Uprimny C, Kroiss AS, Fritz J, Decristoforo C, Kendler D, von Guggenberg E, et al. Early PET imaging with [68]Ga-PSMA-11 increases the detection rate of local recurrence in prostate cancer patients with biochemical recurrence. Eur J Nucl Med Mol Imaging. 2017;44:1647–55. https://doi.org/10.1007/s00259-017-3743-z.
14. Heußer T, Mann P, Rank CM, Schäfer M, Dimitrakopoulou-Strauss A, Schlemmer HP, et al. Investigation of the halo-artifact in 68Ga-PSMA-11-PET/MRI. PLoS One. 2017;12:e0183329. https://doi.org/10.1371/journal.pone.0183329.
15. Wangerin KA, Baratto L, Khalighi MM, Hope TA, Gulaka PK, Deller TW, et al. Clinical evaluation of 68Ga-PSMA-11 and 68Ga-RM2 PET images reconstructed with an improved scatter correction algorithm. AJR Am J Roentgenol. 2018;211:655–60. https://doi.org/10.2214/AJR.17.19356.
16. Lawhn-Heath C, Flavell RR, Korenchan DE, Deller T, Lake S, Carroll PR, et al. Scatter artifact with Ga-68-PSMA-11 PET: severity reduced with furosemide diuresis and improved scatter correction. Mol Imaging. 2018;17:1536012118811741. https://doi.org/10.1177/1536012118811741.
17. Prasad V, Steffen IG, Diederichs G, Makowski MR, Wust P, Brenner W. Biodistribution of [(68)Ga]PSMA-HBED-CC in patients with prostate cancer: characterization of uptake in normal organs and tumour lesions. Mol Imaging Biol. 2016;18:428–36. https://doi.org/10.1007/s11307-016-0945-x.
18. Afshar-Oromieh A, Wolf M, Haberkorn U, Kachelrieß M, Gnirs R, Kopka K, et al. Effects of arm truncation on the appearance of the halo artifact in. Eur J Nucl Med Mol Imaging. 2017;44:1636–46. https://doi.org/10.1007/s00259-017-3718-0.
19. Fennessy N, Lee J, Shin J, Ho B, Ali SA, Paschkewitz R, et al. Frusemide aids diagnostic interpretation of 68Ga-PSMA positron emission tomography/CT in men with prostate cancer. J Med Imaging Radiat Oncol. 2017;61:739–44. https://doi.org/10.1111/1754-9485.12625.
20. Haupt F, Dijkstra L, Alberts I, Sachpekidis C, Fech V, Boxler S, et al. Ga-PSMA-11 PET/CT in patients with recurrent prostate cancer-a modified protocol compared with the common protocol. Eur J Nucl Med Mol Imaging. 2020;47:624–31. https://doi.org/10.1007/s00259-019-04548-5.
21. Afshar-Oromieh A, Sattler LP, Mier W, Hadaschik BA, Debus J, Holland-Letz T, et al. The clinical impact of additional late PET/CT imaging with 68Ga-PSMA-11 (HBED-CC) in the diagnosis of prostate cancer. J Nucl Med. 2017;58:750–5. https://doi.org/10.2967/jnumed.116.183483.
22. Derlin T, Weiberg D, von Klot C, Wester HJ, Henkenberens C, Ross TL, et al. Ga-PSMA I&T PET/CT for assessment of prostate cancer: evaluation of image quality after forced diuresis and delayed imaging. Eur Radiol. 2016;26:4345–53. https://doi.org/10.1007/s00330-016-4308-4.
23. Perveen G, Arora G, Damle NA, Prabhu M, Arora S, Tripathi M, et al. Can early dynamic positron emission tomography/computed tomography obviate the need for postdiuresis image in 68Ga-PSMA-HBED-CC scan for evaluation of prostate adenocarcinoma? Indian J Nucl Med. 2018;33:202–8. https://doi.org/10.4103/ijnm.IJNM_32_18.
24. Uprimny C, Kroiss AS, Decristoforo C, Fritz J, von Guggenberg E, Kendler D, et al. Ga-PSMA-11 PET/CT in primary staging of prostate cancer: PSA and Gleason score predict the intensity of tracer accumulation in the primary tumour. Eur J Nucl Med Mol Imaging. 2017;44:941–9. https://doi.org/10.1007/s00259-017-3631-6.
25. Kruskal WH, Wallis WA. Use of ranks in one-criterion variance analysis. J Am Stat Assoc. 1952;47:583–621. https://doi.org/10.1080/01621459.1952.10483441.
26. Dunn OJ. Multiple comparisons using rank sums. Technometrics. 1964;6:241–52. https://doi.org/10.1080/00401706.1964.10490181.
27. Holm S. A simple sequentially rejective multiple test procedure. Scand J Stat. 1979;6:65–70.
28. Scheirer CJ, Ray WS, Hare N. The analysis of ranked data derived from completely randomized factorial designs. Biometrics. 1976;32:429–34. https://doi.org/10.2307/2529511.
29. R Core Team. R: A language and environment for statistical computing. Austria: Vienna: R Foundation of Statistical Computing; 2018. https://www.r-project.org/
30. Gaertner FC, Beer AJ, Souvatzoglou M, Eiber M, Fürst S, Ziegler SI, et al. Evaluation of feasibility and image quality of 68Ga-DOTATOC positron emission tomography/magnetic resonance in comparison with positron emission tomography/computed tomography in patients with neuroendocrine tumors. Investig Radiol. 2013;48:263–72. https://doi.org/10.1097/RLI.0b013e31828234d0.
31. Silver DA, Pellicer I, Fair WR, Heston WD, Cordon-Cardo C. Prostate-specific membrane antigen expression in normal and malignant human tissues. Clin Cancer Res. 1997;3:81–5.
32. Association WM. World Medical Association Declaration of Helsinki: ethical principles for medical research involving human subjects. JAMA. 2000;284:3043–5.